LANDYNE

User Manual

Stereographic Projection for Interactive

Crystallographic Analysis

Copyright 2011-2025 LANDYNE ©

All Right Reserved

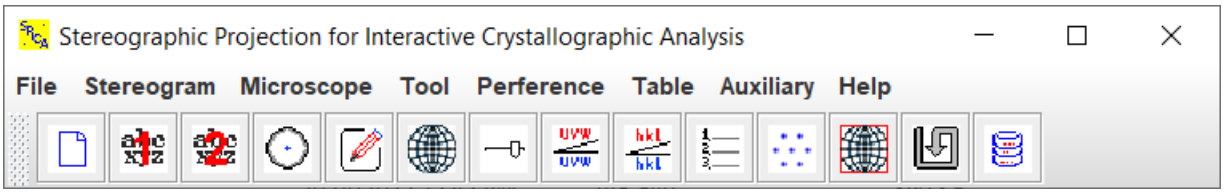

Contents

1. Introduction 2
2. Theory background 3
3. Program design and graphic user interface 7
4. Usage of SPICA4 9
5. Examples 10
6. Installation of SPICA4 14
7. Reference 14

1. Introduction

Stereographic projection involves projecting points from the surface of a sphere onto its equatorial plane. It is particularly significant in crystallography, where a set of points represents directions in three-dimensional space—these directions being lines extending from the sphere's center to the points. A complete set of such projections is commonly referred to as a stereogram. Extensive literature, such as Bennett (1928) and Young & Lytton (1972), details the mathematical foundations and computer implementation of stereographic projection. Moreover, resources on electron microscopy and x-ray crystallography, including works by Edington (1975), Cullity (1978), De Graef (2003), and Fultz & Howe (2008), also cover these aspects comprehensively.

Stereographic projections of crystal directions and planes are usually the essential modules in most commercial or public-domain computer programs for crystallography or electron microscopy; for example, CaRIne (Boudias & Monceau, 1998), Crystallographica (Siegrist, 1997), DIAMOND (Bergerhoff *et al.*, 1996), CrystalMaker (Kohn, 2007), Crystal Studio (Crystal Studio, 2015), WebEMAP (Zuo & Mabon, 2004) and JEMS (Stadelmann, 1987). As program modules, they are sufficient for regular use to draw stereograms of crystal directions and planes; on the other hand, dedicated computer programs are available for the extended usages of the stereographic projections. A computer program for simulation of electron

diffraction Kikuchi pattern was developed by Lee *et al*. (1994) based on the work by Young & Lytton (1972). JECP/SP (Li, 2004) was developed for generating stereographic projections, applicable to specimen orientation adjustment in transmission electron microscope (TEM) experiments. SP2 (Chen & Chen, 2012) was developed for standard operation of stereographic projections and can also be used to make composite stereograms, which are necessary to explore the orientation relationships between two crystalline phases.

In the realm of electron diffraction experiments for crystallographic analysis, stereographic projection software is expected to encompass more than just standard stereogram analysis. Advanced functionalities include generating composite stereograms to analyze relationships between different crystalline phases, simulating Kikuchi maps, and predicting tiling angles in selected-area electron diffraction (SAED) experiments.

SPICA4 represents a significant advancement in this field, offering these comprehensive features and more. Developed to cater to both educational needs in crystallography and practical requirements for TEM researchers, SPICA4 serves as a versatile tool. It supports teaching by aiding students in understanding crystallographic concepts and serves as a robust instrument for researchers engaged in TEM experiments, facilitating the analysis and interpretation of experimental results effectively.

2. Theory background

As mentioned above, the mathematics behind the geometry of stereographic projection can be found in most books for electron microscopy and x-ray crystallography. There are various ways to implement stereographic projections in computer programs. The implementation of SPICA4 is briefly described in this section.

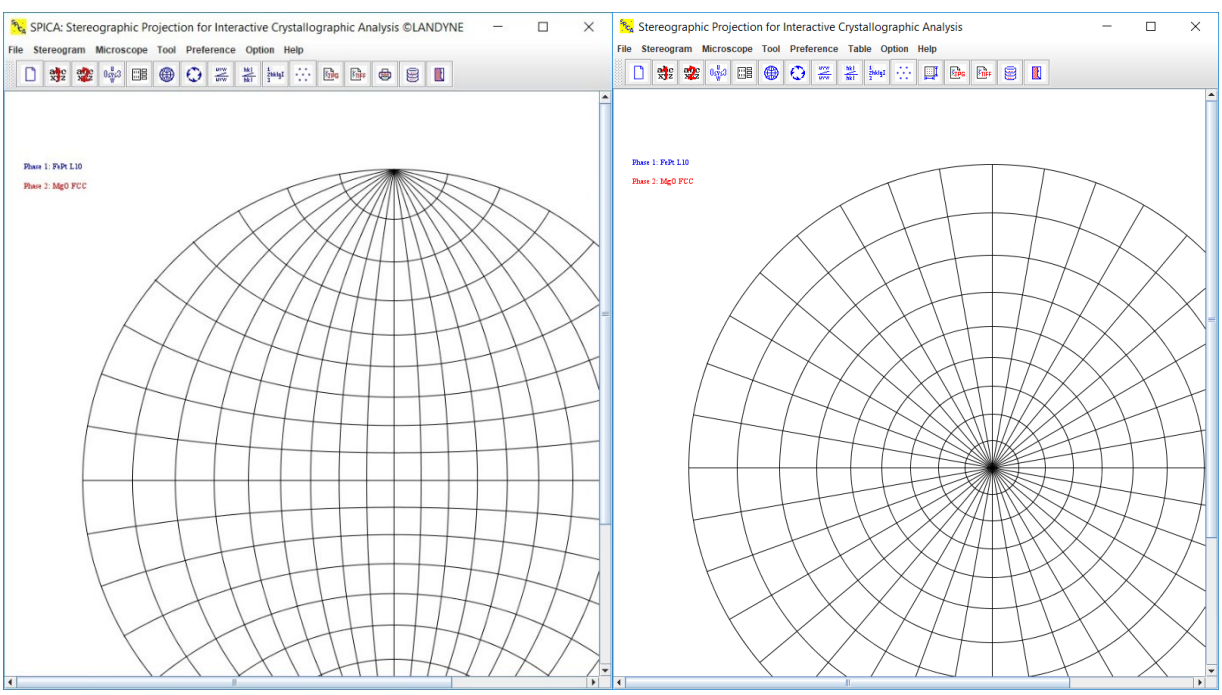

Figure 1. The graphic user interface of SPICA4 with (a) the Wulff net and (b) a symmetric net.

2.1 Wulff net

Wulff net, or stereographic net, is a stereographic projection of the longitude and latitude curves on a sphere, which can be drawn as two series of circles with their center and radius shown in Figure 3.

Longitude arcs:

$$y^2 + (x \pm r/\tan(\varphi))^2 = (r/\sin(\varphi))^2 \qquad (1a)$$

Latitude arcs:

$$(y \pm r/\cos(\theta))^2 + x^2 = (r \cdot \tan(\theta))^2 \qquad (1b)$$

Here r is the radius of the sphere of a stereogram. The coordinate (x, y) is on the longitude or latitude circles. The above formulas can be derived based on the definition of the Wulff net.

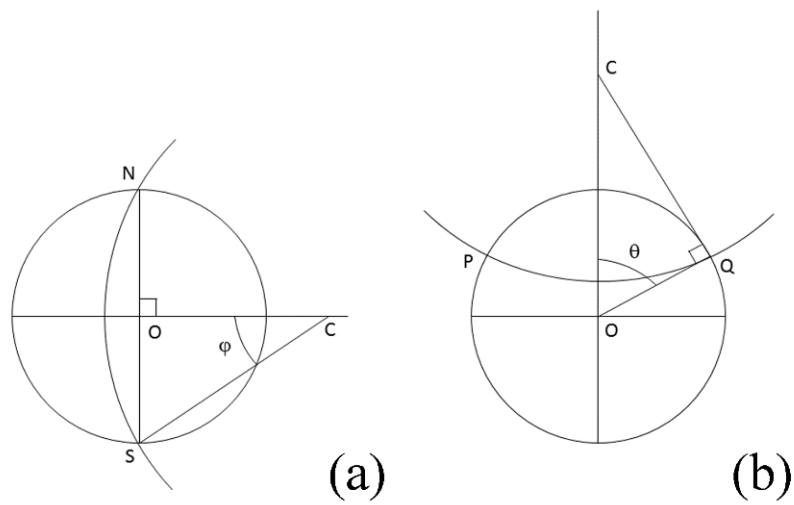

Figure 2. The construction of the Wulff net: (a) the longitude and (b) the latitude curves on a sphere.

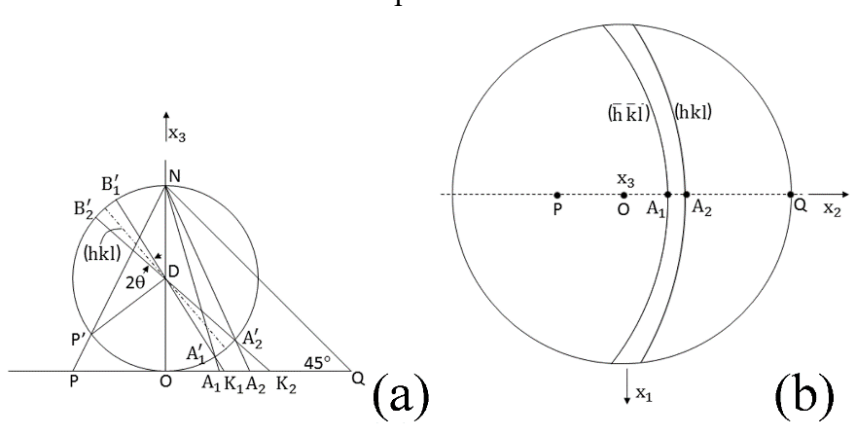

Figure 3. The geometric construction of a Kikuchi map by stereographic projection.

2.2 Stereographic projection

The Cartesian coordinate system for a crystal lattice is set up as follows: the *c* axis of a crystal lattice is set up along the *z* axis of the coordinate system, the *a* axis is set up in the *x-z* plane, and then the coordinates of the *a* and *b* axes are fixed up. A stereogram is firstly calculated using (001) or [001] as an initial direction of projection. The stereogram with a specific direction of projection, (hkl) or [uvw], is obtained by rotating the initial stereogram so that (hkl) or [uvw] becomes the direction of projection.

Figure 4 (a) shows a sphere with its center at D and a plane passing through O for stereographic projection. The projection from the north pole and through the equator of the sphere to the stereographic plane is NQ. It defines a circle with a radius of OQ on the stereographic plane. For any point P on the stereographic plane, a line NP intersects the sphere at one point P'. It defines the stereographic projection of P' to P on the stereographic plane. In Cartesian coordinates, the (x, y, z) on the sphere and the (X, Y) on the plane, the relation of the projection point on the stereographic plane and the associated point on the sphere are given by the formula,

$$(X, Y) = \left(\frac{x}{1-z}, \frac{y}{1-z}\right) \qquad (2)$$

where the set of points (x,y,z) are on the unit sphere, so that $x^2 + y^2 + z^2 = 1$.

2.3 Composite stereogram

SPICA4 allows two stereograms either from the same or different crystalline phases to be generated simultaneously; either the two single stereograms or the overlain stereogram can be displayed separately. Both stereogram and the Wulff net can be rotated in an increment step of 0.01° to analyze the crystallographic relationship. If the stereograms are generated from the same crystalline phase, different properties can be displayed, e.g., one with the selected plane indices shows trace curves, and the other shows the standard plane indices; one shows the plane (hkl) pole and other shows the [uvw] poles, or one shows Kikuchi map and the other shows the [uvw] poles.

2.4 Kikuchi map and trace curve

Although the Kikuchi patterns obtained using a TEM are not truly stereographic projections, they are excellent approximations to it when the camera length is relatively large. Furthermore, the use of stereographic projection in simulated patterns allows the display of all possible orientations on a single figure, which cannot be done easily with a photographic montage.

The coordinate system for generating the Kikuchi map in stereographic projection was adopted the work by Young & Lytton (1971). The geometry for the standard stereographic projection of a Kikuchi line pair is shown in Figure 3; (b) is the projection of (a) with the observer looking from N toward O. Here the projected plane-normal $P(P_x, P_y)$ can be calculated from the following equations,

$$P_x = (2DO)\tan\left(\frac{1}{2}\gamma\right) P'_x / (P'^2_x + P'^2_y)^{\frac{1}{2}} \quad (3a)$$

$$P_y = (2DO)\tan\left(\frac{1}{2}\gamma\right) P'_y / (P'^2_x + P'^2_y)^{\frac{1}{2}} \quad (3b)$$

$$\gamma = \cos^{-1}[P'_z/(P'^2_x + P'^2_y + P'^2_z)^{\frac{1}{2}} \quad (3c)$$

where P'_x, P'_y, and P'_z are the coordinates of P' ($r = (P'^2_x + P'^2_y + P'^2_z)^{\frac{1}{2}}$) referred to the standard basis for stereographic projection, and γ is the angle between the plane normal to DP' and DO. The formulas above can be used to generate trace curves by applying $\theta = 0°$.

The Kikuchi map is generated from the data set of the (h k l) stereographic projection, and the distribution of the zone axes on the Kikuchi map can be found from the [u v w] stereographic projection of the same crystal phase on the second stereogram. In order to draw the trace lines, we need to know the plane-normal index. For a cubic crystal, a plane normal is parallel to the orientation with the same index as this plane, but it is necessary to transform between the plane index and the plane-normal index for non-cubic crystals. A function for the transformation from a plane (h k l) to the plane-normal [u v w] is provided in SPICA3 based on the matrix by (Liu & Liu, 2012).

2.5 Prediction of the tilt or rotation angles for a TEM holder

Computer-assisted specimen orientation adjustment in TEM experiments is possible for a crystalline specimen with known lattice parameters. The microscope can be kept in the image mode while the specimen is tilted to any zone axis within the range available for the TEM specimen holder under calculated guidance. Chou (1987) described an application of stereographic projection for specimen orientation adjustment. A slightly different algorithm was adopted in JECP/SP and inherited in SPICA4.

The critical point is to set up the positions of the TEM specimen holder and the crystal orientation in the stereographic projection sphere. The tilt angle of the TEM goniometer and the second tilt angle are assumed to be along longitude and latitude of the stereographic projection sphere. The crystal orientation can be obtained from the observed SAED pattern. Suppose that the SAED pattern with a zone axis [uvw] is currently observed. For any diffraction spot (hkl) on the SAED pattern, the azimuth χ is between the line of (000)-(hkl) and the projection of the TEM specimen holder (or goniometer axis) on the fluorescent screen, as shown in Figure 4. A stereographic projection map can be calculated using the above input parameters to provide all the zone axes with computer-predicted tilting or rotating angles. The tilting limitation of the TEM holder can also be drawn in the generated stereogram.

2.6 Modules for crystallographic calculation

One module mentioned above is for the transformation from the crystal plane (h k l) to the plane-normal [u v w] for non-cubic crystalline phases. Other modules include the calculation of the angles between two crystal planes, between two zone axes or between a plane-normal and a zone axis, the transformation between Miller and Miller-Bravais indices for the hexagonal system, and a calculated list of reflection (hkl), together with the plane spacing and the kinematical intensity.

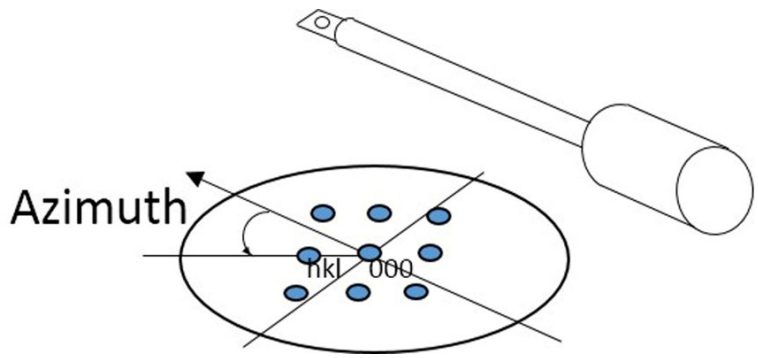

Figure 4. The geometric relation of the observed SAED pattern and the TEM specimen holder for a stereographic projection as guidance in SAED experiments.

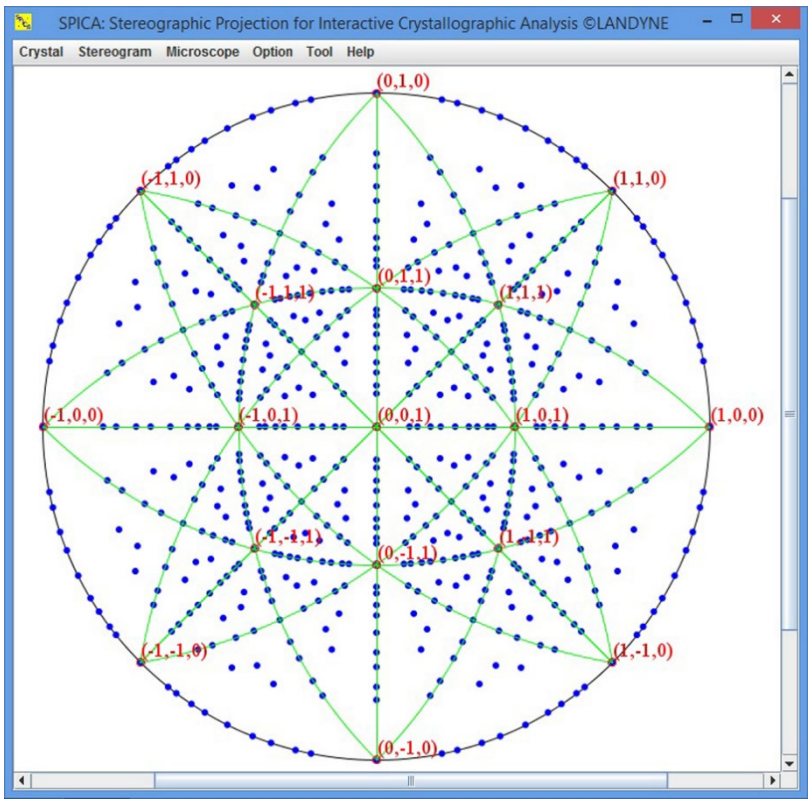

Figure 5. SPICA4 with an (hkl) stereogram of a cubic structure as an example.

3. Program design and graphic user interface

SPICA4 was developed using openJDK21 and has undergone successful testing on Microsoft Windows OS versions 10 and 11. The software is versatile, capable of functioning both as a standalone program and as an integrated component within the Landyne software package, which includes a launcher. Interested users can download SPICA4 and the associated components from https://www.unl.edu/ncmn-enif/xzli/computer-programs.

The graphical user interface (GUI) of SPICA4 leverages Java Swing to create a familiar Windows-style operational environment. It features a scalable display panel for stereograms and includes various dialogs for tasks such as data input/output and graphic editing operations. Figure 1 illustrates the SPICA4 interface, showcasing a menu bar and an example of a cubic (hkl) stereogram with prominent trace lines.

Figure 2 depicts three essential operational dialogs within SPICA4: (a) the calculation dialog, (b) the pole range dialog, and (c) the orientation dialog for Wulff net and stereograms. SPICA4 offers additional operational dialogs for various purposes, although they are not shown here. Users have the flexibility to adjust the frame size, including the display panel, to suit their preferences and operational needs.

SPICA4 is a fully functional tool for generating stereograms of crystal directions and planes. To generate a stereogram, the user needs to provide the crystalline lattice parameters, *a, b, c, α, β, γ,* and the direction of projection, [*uvw*] or (*hkl*). As an option, the Wulff net can be drawn and rotated on top of the generated stereogram. Crystal lattice parameters can be loaded from a data file and readjusted in the calculation dialog (see Figure 2(a)). Two stereograms from two crystalline phases can be generated and overlain into a composite stereogram for analyzing their structural relationship. The list of (hkl) can be edited to show trace curves of selected (hkl) poles. Kikuchi maps can be displayed from the generated data of (hkl) poles and the wavelength of the incident beam. The zone axes for the Kikuchi maps can be generated from the same crystalline phase on the second stereogram and then overlaid with the Kikuchi map. The additional application is to predict tilt/rotation angles of zone axes for both double and rotation TEM holders.

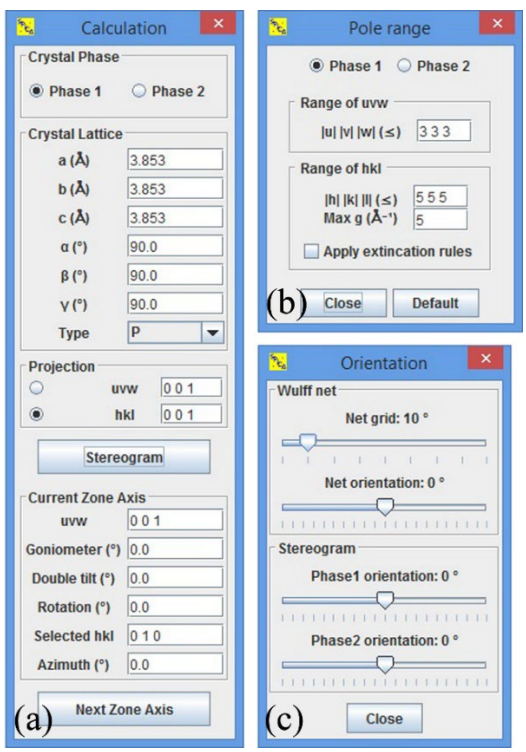

Figure 6. Three basic operational dialogs in SPICA4, (a) the calculation dialog, (b) the pole range dialog and (c) the orientation dialog for Wulff net and stereograms.

4. Usage of SPICA4

SPICA4 is coded mainly in Java and partially coded for PC with Microsoft Windows only. To run the software, openJDK21 or higher must be installed on a PC. The executable bytecodes of Landyne suite (including the SPICA) is available at https://www.unl.edu/ncmn-enif/xzli/computer-programs.

Uncompress the installation file landyne6.z7 in a selected directory and use the Landyne launcher and then select the SPICA.

The basic step for using SPICA is listed below,

- FePt L10 and MgO FCC as default input lattices for phase 1 and phase 2.
- The crystal lattice can be loaded from Crystal/phase and modified via input fields.
- Click Calculation/Stereogram to generate a stereographic projection map.
- Click the right mouse button to modify the display options.
- Calculate hkl stereogram and click mouse right button to select Show trace for display.
- Calculate hkl stereogram and select Show Kikuchi to display Kikuchi map.
- Load the other the same phase and calculate uvw to display zone axes.
- Press the left-mouse-button and drag to zoom the stereogram.
- Hold Ctrl and click the left mouse button to set the viewpoint center.
- Click the stereogram/pole list, to remove the selected poles or to add on new poles.
- Click stereogram/orientation, Wulff net and stereograms can be rotated.
- The overlaid stereographic projections give the crystallographic relation of two phases.
- Click Calculation/Goniometer to generate TEM holder information.
- Click Option to change color, label size and tilt label.
- Click Tool to calculate the angle of two [uvw]s or two (hkl)s.
- Click Help/Current drive to obtain the serial number of the current driver.

More details on i) a (hkl) stereographic map with selected trace lines and ii) a Kikuchi map with the index of zone axes. It is easy to create a (hkl) stereographic map, and to combine selected trace-lines by selecting the same phase as the second phase. It is usually to adjust the range of hkl first and then use the mouse-right-button to select the trace lines. It is easy to create a Kikuchi map and to combine indices of the zone axes by selecting the same phase as the second phase and work on the [uvw] stereographic map.

Although only lattice parameters are involved in the SPICA, we usually use the crystal structure file for Landyne suit as the input file. A new crystal structure data file can be prepared using the **New Crystal Structure File** dialogue window (more details see SVAT). The dialogue window provides an automatic assistant for the user and makes sure to meet the requirement of the file format. The template is embedded with the 230 space groups in the Hermann-Mauguin notation, which list in the international table for crystallography. To save the data structure, click the **Save** button; or make a new one click the **New** button.

The crystal file can be also converted from previous data for modification or from a crystallographic information file (CIF). If a data file in an alternative setting of space group for triclinic, monoclinic and orthorhombic systems is used, please click on the alternative settings (1~74). A tool for the transformation of files in the nonconventional notations to the standard notations is provided.

5. Examples

Some application examples are given here to show the proof of validity and practicability of SPICA4. The necessary usage steps are introduced here, and more details are given in the user manual of SPICA4.

5.1 Stereogram and Wulff net

The input parameters to generate a stereogram include the lattice parameters of a crystalline phase and a direction of projection. The lattice parameters can be loaded using the menu bar from the input file of a crystal structure, and the lattice parameters can be readjusted in the calculation dialog, if necessary. The range of the poles is controlled by a set of preset values in the pole range dialog. When a list of the poles is generated, the pole in the list can be deleted, or a new one can be added to the list. The stereogram and the Wulff net can be rotated separately. The display of the stereogram can be zoomed in or out. Figure 6 shows (a) the (h k l) stereogram and (b) the [u v w] stereogram of the hexagonal structure of Zn, a = 0.26649 nm, b = 0.226649 nm, c = 0.49468 nm, α = 90°, β = 90° and γ =120°. In order to display all indices clearly, the maximum indices were chosen as h≤2, k≤2, l≤2, u≤3, v≤3 and w≤1. The Miller index was labelled in the stereogram; the Miller-Bravais index can be transformed from Miller index using a module in SPICA3. Wulff net, as a tool for measurement, can be applied to the stereogram by users. Wulff net is applied in Figure 1 and not applied in Figure 6.

5.2 Composite stereogram

An example is taken from our recent work on $Mn_2CrGa_{1-x}Al_x$ alloy, x=0.0, 0.2, 0.5 (Li *et al*., 2016). Spinodal decomposition of the alloys (x=0.2, 0.5) generates two crystalline phases with a fixed orientation relationship after annealing treatment at 500 °C for 2 hrs. The lattice parameters of the two phases in $Mn_2CrGa_{0.5}Al_{0.5}$ alloy are listed in Table 1. Figure 8 (a) shows a TEM image of the two crystalline phases in $Mn_2CrGa_{0.5}Al_{0.5}$ alloy, the cubic phase in light grey has a composition of $Mn_{63}Cr_{11}Ga_{13}Al_{13}$, and the tetragonal phase with strip shape in dark grey has a composition of $Mn_{45}Cr_{31}Ga_{13}Al_{11}$. Figure 8 (b-d) shows the SAED patterns to reveal the orientation relationship of the two crystalline phases. Figure 9 shows the composite stereograms of (a) the index labels on the cubic phase and (b) the index labels on the tetragonal phase. The fixed orientation relationship of the two crystalline phases are,

$$(001)_t \,//\, (100)_c \qquad [100]_t \,//\, [012]_c \qquad [310]_t \,//\, [011]_c \qquad [120]_t \,//\, [010]_c$$

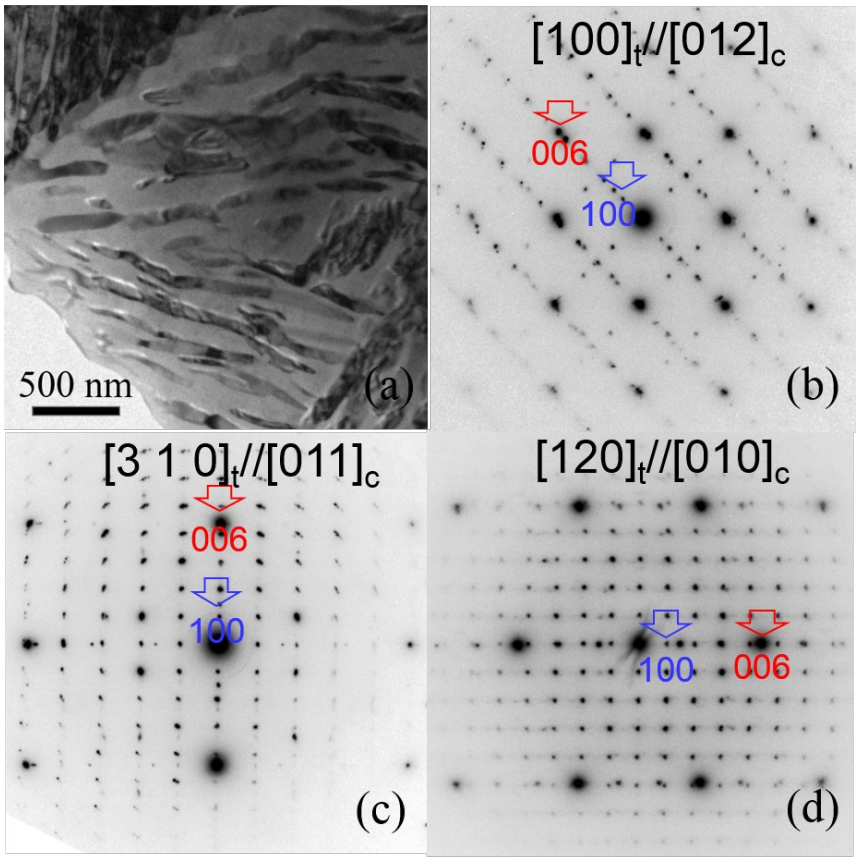

Figure 7. Two crystalline phases in $Mn_2CrGa_{0.5}Al_{0.5}$ alloy as the result of a spinodal decomposition: (a) a TEM image of the two phases, cubic phase in light grey and tetragonal phase with strip shape in dark grey, and (b-d) the electron diffraction patterns taken from the two crystalline phases.

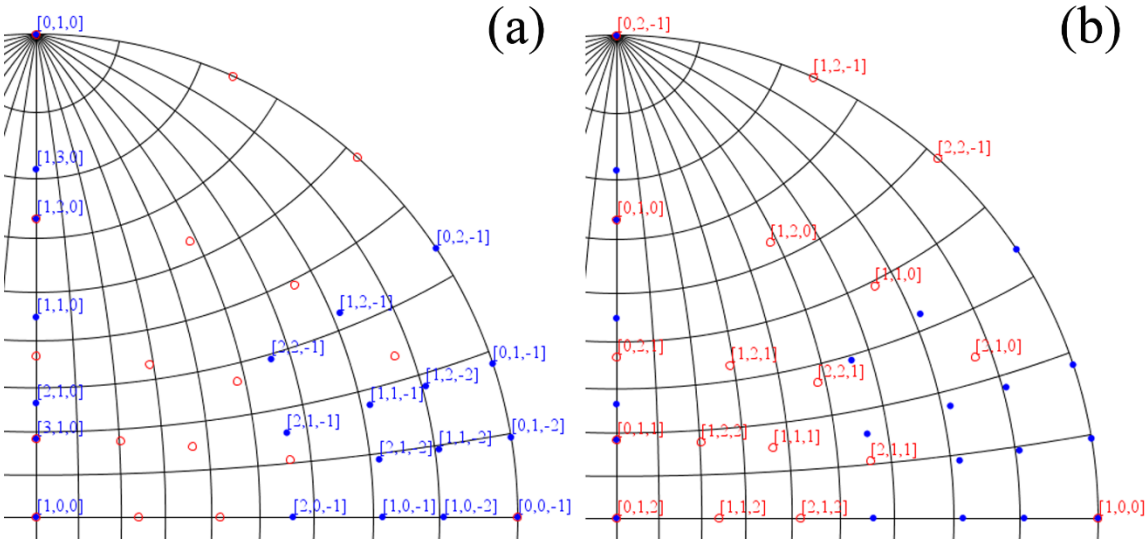

Figure 8. Composite stereogram with (a) the index labels for the cubic phase and (b) the index labels for the tetragonal phase.

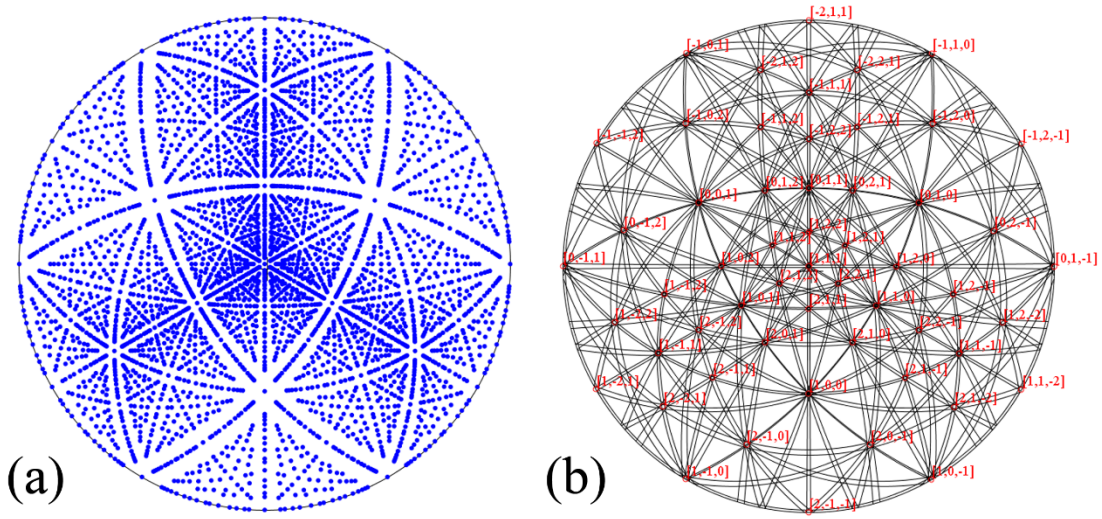

Figure 9. Kikuchi maps of a primitive cubic structure with [111] zone axis in the center, (a) generated using the method described by Liu & Liu (2012) and (b) generated using the formula by Young & Lytton (1971) with the wavelength of 0.0251 Å (200kV).

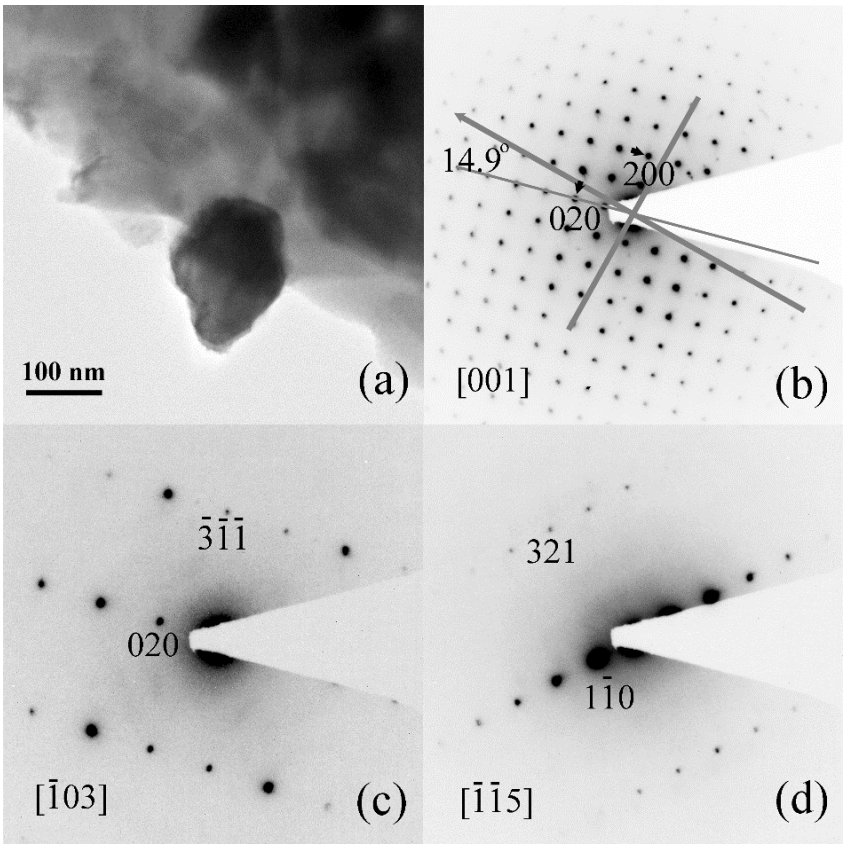

Figure 10. A new tetragonal phase in Co-Fe-Cr-Ge alloy. (a) TEM image of the tetragonal phase with the grain size about 150 nm, (b-d) the SAED patterns of the tetragonal phase.

5.3 Kikuchi map and trace curve

The Kikuchi map is displayed by first generating a stereogram of (h k l) and then selecting the corresponding display mode in SPICA4. The additional parameter for the Kikuchi map is the wavelength of the incident beam or the high voltage on TEM. Figure 10 shows the Kikuchi maps of a primitive cubic structure with the [111] zone axis in the center, (a) generated using the method described by Liu & Liu (2012) and (b) generated using the formula by Young & Lytton (1971) with the wavelength of 0.0251 Å (200kV). The overlain distribution of the [uvw] zone axes is shown in Figure 10(b) as the result of a composite stereogram.

Like the Kikuchi map, the Kossel map in x-ray diffraction and the electron backscatter diffraction (EBSD) map can also be simulated with SPICA4 by selecting an appropriate wavelength. The trace curve is displayed by generating a stereogram of (h k l) and then selecting the corresponding mode; one example was shown in Figure 1.

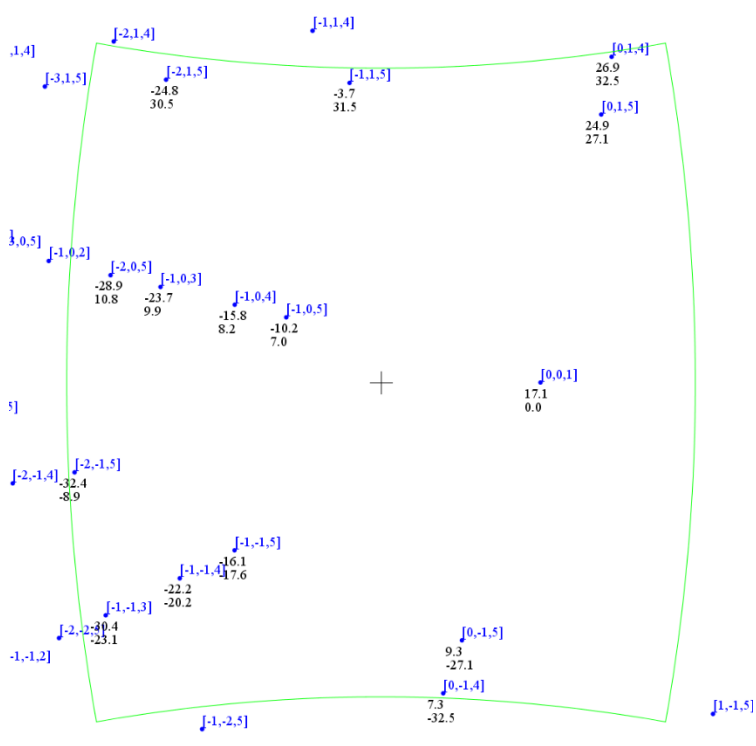

Figure 11. A new tetragonal phase in Co-Fe-Cr-Ge alloy as an example using SPICA4 to predict the tilt angles for all zone axes within the tilt limitation of the TEM specimen holder. Two of the SAED patterns of $[\bar{1}03]$ and $[\bar{1}\bar{1}5]$ zone axes were selected and displayed in Figure 10 (c) and (d).

5.4 Tilt-angle prediction for a TEM holder

This function is beneficial in many situations. For example, (a) when a severely stained specimen is observed, and the visibility of Kikuchi line pairs is thus inadequate. (b) When a

beam-sensitive specimen is examined, it is essential to shorten the time spent on specimen tilting while the electron beam is on the specimen area of interest. (c) When a small grain-size specimen is investigated, for which even a slight orientation adjustment may cause the corresponding diffraction pattern to disappear due to a lateral sample shift. (d) When a crystalline specimen is used in acquiring electron diffraction intensities of reachable zone-axis patterns for structure determination.

An example is the electron diffraction experiment on a new tetragonal phase in the composition of $Co_{39}Fe_{42}Cr_9Ge_{10}$ in our recent work (Jin *et al*., 2016). The lattice parameters are listed in Table 1. Figure 10 (a) shows a TEM image of the new tetragonal phase with a grain size of about 150 nm, and Figure 11 (b-d) shows SAED diffraction patterns of the new tetragonal phase. In the experiment, the [001] SAED pattern in Figure 11(b) was obtained at tilt angles of (17.1°, 0.0°) with a double-tilt TEM holder. The angle between the vector (000)-(010) and the holder axis is about 14.9°. Figure 12 was generated using SPICA4 with the above parameters to predict the tilt angles for all zone axes within the tilt limitation of the TEM holder. The TEM specimen was tilted according to the predicted tilt angles, and all SAED patterns were obtained. Two of the SAED patterns of $[\bar{1}03]$ and $[\bar{1}\bar{1}5]$ zone axes were displayed in Figure 11 (c) and (d). The forbidden reflection, e.g. (010), in Figure 11 (c) appears in Figure 11(d) due to the double diffraction effect.

6. Installation of SPICA4

6.1 Installation

Download and install the most recent OpenJDK from the internet. Create a dedicated fold for LANDYNE software suit. Copy and decompress the package. If users have a license file, copy the license to the programs folder. Click the SPICA3 in Landyne launcher to start the software.

6.2 Get a license

A license file is needed to unlock the program for loading new file data. Without the license file, the program is locked up in demo mode. A license can be purchased from LANDYNE computer software.

7. Reference

Bennett, T. (1928). *The American Mathematical Monthly*, 35, 24-27.

Bergerhoff, G., Berndt, M. and Brandenburg K. (1996). J. Res. Natl. Inst. Stand. Technol. 101, 221-225.

Boudias, C. & Monceau, D. (1998). CaRIne Crystallography. Verison 3.1. Software CaRIne Crystallography, Senlis, France.

Burgers, W. (1934). *Physica*, 1, 561-586.

Chou, C.T. (1987). *J. Elec. Micros. Tech*. **7**, 263-268.

Cullity B.D. (1978). *Elements of X-Ray Diffraction*, Addison-Wesley, London.

Crystal Studio (2015). http://www.crystalsoftcorp.com.

De Graef, M. (2003). *Introduction to Conventional Transmission Electron Microscopy*, Cambridge University Press.

Edington, J.W. (1976). *Electron Diffraction in the Electron Microscope*, The Macmillan Press Ltd.
Fultz, B. and Howe, J. (2008). *Transmission Electron Microscopy and Diffractometry of Materials,* Springer.
Jin, Y.L., Li, X.Z., Kharel, P., Shah, V.R., Skomski, R., and Sellmyer D.J. (2016). A New Tetragonal Phase in Co-Fe-Cr-Ge Alloy, to be published.
Kohn, S. C. (2007). Terra Nova, 7, 554–556.
Lee, W.-B., Park, C.-R., Park, C.-G. and Chun, C.-H. (1994), Korean J. Electron Microsc. 24, 115-122.
Li, X. Z. (2004). *J. Appl. Cryst*. **37**, 506-507.
Li, X.Z., Zhang, W.Y. and Sellmyer D.J. (2016). A TEM Study of the Spinodal Decomposition in $Mn_2CrGa_{0.5}Al_{0.5}$ Alloy, to be published.
Liu, H. and Liu, J. (2012). *J. Appl. Cryst*. 45, 130-134. .
Siegrist, T. (1997). J. Appl. Cryst. 30, 418–419.
Stadelmann, P. (1987). Ultramicroscopy, 21, 131–146.
Young C.T. and Lytton J.L. (1972). *J. Appl. Phys*. **43**, 1408-1417.
Zuo, J.M. & Mabon, J.C. (2004). Microsc. Microanal. 10, 1000–1001.